Advances in Science and Technology Research Journal

Advances in Science and Technology Research Journal 2024, 18(5), 342–360
https://doi.org/10.12913/22998624/190483
ISSN 2299-8624, License CC-BY 4.0

Received: 2024.06.04
Accepted: 2024.07.20
Published: 2024.08.01

Determination of Hole Blocking Conditions for Perforated Sifting Surfaces

Serhii Kharchenko[1*], Sylwester Samborski[1], Farida Kharchenko[2], Ihor Kotliarevskyi[2]

[1] Lublin University of Technology, ul. Nadbystrzycka 36, Lublin, 20-618, Poland
[2] Sumy National Agrarian University, ul. Herasyma Kondratieva 160 Street, Sumy, 40000, Ukraine
* Corresponding author's e-mail: s.kharchenko@pollub.pl

ABSTRACT

The efficiency of widespread technological processes of sieve sifting of loose materials depends on timely cleaning of holes from the blocked particles. The blocking of holes occurs under specific conditions related to mechanical-and-physical properties of loose material particles, constructive and technological parameters of perforated sifting surfaces and clean-up systems. We established the conditions that contribute to blocking of holes of sifting surfaces and identified all significant factors, namely size, mass, constant of friction and Young's modulus for loose material particles; form and size of hole, thickness of perforated surface; loose material layer thickness and velocity. Using analytical and experimental methods, we identified variation range of these factors for loose material particles of biological origin, such as buckwheat, wheat, peas, corn. As a result of this study, we received analytical equations for determination of force of adhesion of loose materials particles with the edge of holes of perforated surfaces. The numeric calculations allowed establishing the dependence of the force of adhesion on moisture and thickness of loose material layer, as well as thickness and shape of the holes of the perforated surfaces. We have also established the dependence of constant of friction, mass, Young's modulus from the moisture of particles of loose material. The obtained results make it possible to determine the force of adhesion and prediction the power necessary for unblocking this hole, created by the cleaning system elements, such as brushes and elastic impact cleaners. The use of this method will make it possible to justify the parameters of the system for cleaning holes of perforated sifting surfaces with different types of holes and when separating different types of loose materials.

Keywords: blocking, hole, perforated surface, sifting, loose materials, force of adhesion.

INTRODUCTION

The processes of separation of loose materials particles are present in a large number of technological processes of construction, mining, chemical, pharmaceutical, agricultural, food and other industries [1, 2]. The separation of loose materials particles is carried out on perforated sifting surfaces (PSS), where the components are separated by size. The process task is separation of loose material in two components (fractions): passing fraction that was sieved through the holes; tailing fraction left on the perforated surface. In the process of sifting the particles of loose material contact with the edges of PSS holes and if the size is similar they are blocked. The efficiency of the process of loose medium separation depends on constructive and kinetic PSS parameters and features of the components. The intensity of sifting of loose medium particles is determined by vibration: frequency and amplitude of forced vibrations of perforated surfaces [3, 4]. The constructive PSS parameters, such as location pitch, size and shape of the holes and bridges, not only regulate the penetration coefficient (cross-sectional area), but also the conditions for orientation and activation of sifting of particles of loose medium [5, 6]. The use of PSS with holes of complex geometry [4, 7] enables to increase the sifting efficiency of components for 30–90 %, comparing

to PSS with basic round, rectangular or triangular holes. The PSS operating efficiency depends on timely cleaning of holes from the obstructed particles of loose material. The holes clogging leads to decrease in the penetration coefficient of the perforated surface, which causes a decrease in the productivity of the separation equipment.

Technical systems in the form of [8–10] elastic impact cleaners, brush cleaners, impact mechanisms, pneumatic cleaning, scraping devices, are used for PSS holes cleaning.

Ball elastic impact cleaners [8, 9], which under the influence of their own mass and velocity, knock out stuck particles of the loose medium from the PSS holes (Fig. 1) have become widespread. The velocity of ball elastic cleaners (position 3, Fig. 1) is ensured by the contact with the bumper (position 4, Fig. 1), which is vibrating with the PSS (position 2, Fig. 1). The bumper is located under PSS and consists of sidewalls and foundation that create meshes. The bumper does not provide resistance to the passage of particles of the loose medium of the passing fraction, but keeps the elastic balls in the mesh. Rigid mounting of the bumper on the PSS allows us to use its vibration without additional devices and energy consumption. The efficiency of sifting of loose medium particles depends on timely cleaning of vibrating PSS holes with the help of elastic balls impact impulses.

The factors that influence the efficiency of PSS holes cleaning are [11, 12]: quantity, mass, size and elastic features of balls; bumper parameters; PSS parameters; characteristics of loose material particles. The cleaning system efficiency criterion can be a clogging coefficient [13, 14]:

$$\delta = \sum n_b / \sum n_h \tag{1}$$

where: n_b is a number of clogged (blocked) holes;
$\sum n_h$ is total number of PSS holes.

The coefficient δ is variable by time and characterizes the intensity of $d\delta / dt$, which depends on efficiency of elastic balls action and conditions of holes clogging. The influence of number of blocked holes on the efficiency of sifting of loose medium particles can be expressed through the expression of the active sifting area:

$$S_a = \delta S_{ps} k_p \tag{2}$$

where: S_{ps} – is PSS area; k_p – penetration coefficient (cross-sectional area):

$$k_p = \frac{\sum S_h}{S_{ps}} \tag{3}$$

where: $\sum S_h$ – the area of all holes on the perforated surface.

The negative impact of hole clogging on technological performance indicators of separation equipment is considered in [15, 16].

Simultaneously with the process of holes clogging occurs the reverse process of their unblocking and sifting of particles of loose material takes which requires comprehensive consideration [17]. The scientists are interested in holes clogging conditions that are based on correlation of force of adhesion of particles of loose medium with the edge of the hole and wedging force created by kinetic energy of elastic ball impact. The correlation of these forces is determined by the intensity of PSS holes cleaning. It should be noted that the character of holes clogging depends on the correlation between the size of holes and separating size of particles of loose material of passing fraction [11] that proves their necessity in study. The objectives of this study are determination of conditions of clogging (blocking) of holes, characterized as PSS parameters, and characteristics of particles of loose materials, that are the source data for optimization of PSS cleaning system with impact elastic ball cleaners.

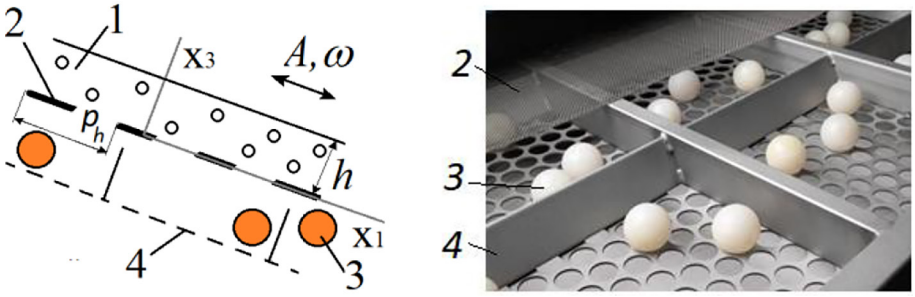

Figure 1. Holes cleaning system: 1 – particles of loose material; 2 – perforated sifting surface; 3 – ball cleaner; 4 – bumper

RESEARCH METHODOLOGY

The intensity of holes clogging depends on the kinematic (frequency and amplitude of vibrations) and structural (size and shape of holes and bridges, edge parameters, surface thickness and angle of inclination) parameters of the vibrating PSS, as well as on the physical and mechanical properties of loose material particles (shape, size, density, coefficient of elastic directional deformation), which together determine the value of the force of adhesion. The force of adhesion between the particles and the edge of the hole reaches significant values that can exceed the mass of the particles by 100 or more times [18, 19]. It proves the necessity to take such forces into account when forming hole clogging conditions at design calculations and scientific studies of PSS operating efficiency.

Before the study, we make the following assumptions [12]:

- PSS has a flat rectangular plate shape with holes in the form of: a circle with a diameter of ($d_h = 2R_h$) and an equilateral triangle with a leg (l_h);
- the shape of the loose material particle is modeled as an ellipsoid of rotation or tetrahedron with the following external dimensions: length (L), width (W) and thickness (T);
- the force of adhesion is the resultant of all forces that holds a particle of loose material in the hole;
- the holes have an edge located at right angles to the PSS working plane.

The hole cleaning condition is formed from the correlation of the adhesion force of the loose material particle with the edge of the holes (F_{ad}) and the kinetic energy of the ball, which forms the unblocking force (Fig. 2) [20, 21]:

$$\frac{m_b V_{rb}^2}{2} \geq F_{ad} \Delta l \tag{4}$$

where: m_b, V_{rb} – mass and relative velocity of the elastic ball of the cleaner; Δl is the length of the clogging path of a loose material particle relative to its center of gravity.

The most difficult among the components of the hole cleaning condition, is the right part of the equation, the value of which varies depending on the PSS parameters and the properties of the loose material. The main task of this study is the development of a method for identifying the force of adhesion F_{ad} and clogging paths l of loose material particle. Taking into account the significant factors of the clogging process, we developed a method for determining the adhesion force, which consists of the following stages:

- experimental determination of the properties of loose medium particles, such as elastic coefficient (Young's modulus), dimensional characteristics, constant of friction, moisture;
- processing of experimental results and determination of the dependences of the elastic modulus, mass and coefficient of friction of loose material particles on their moisture;
- analytical determination of the adhesion force with calculation of the pressure on the surface of contact of the particle with the edge of the PSS hole;
- processing of results and determination of the dependence of the adhesion force on PSS parameters and properties of loose material particles.

These studies have been conducted for a specific type of hole cleaner - free-moving and impact-actuated elastic balls. The effectiveness of other cleaners, such as fractional brush cleaners, also requires a determination of the cohesive force. The difference will be the introduction of brush parameters that will determine the ejection force. Thus, the proposed methodology for determining the unlocking condition is universal and can be used for other types of cleaners. The determination of the force of adhesion of the loose material particle with the edges of the PSS hole will allow us to rationally justify the parameters of the cleaning system, including optimization of the parameters of the balls and the bumper, which will increase the efficiency of the separation equipment.

EQUIPMENT AND MATERIALS

The main components of experimental studies were laboratory equipment, elastic balls, particles of loose materials and PSS.

Elastic ball cleaners

For the study we used ball cleaners (Fig. 2) made of natural NR-type rubber with the following parameters (Table 1), which correspond to known studies [22, 23].

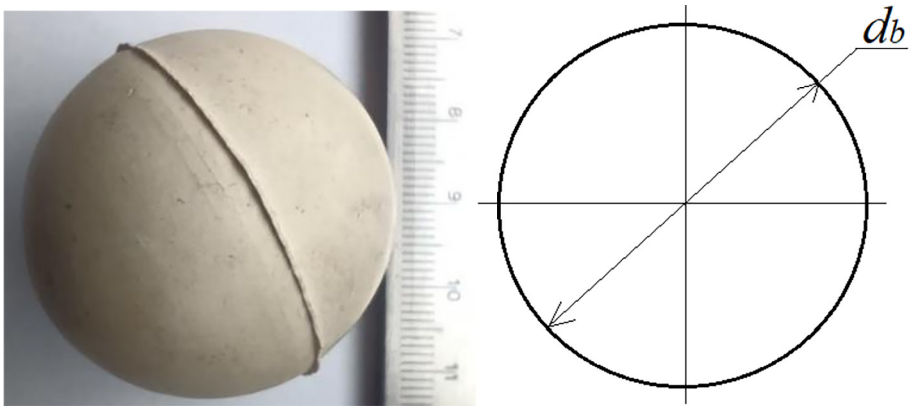

Figure 2. General view and diagram of ball cleaners

Table 1. Parameters of ball cleaners (average values)

Parameters	Value
Diameter, mm	35
Density, g / cm^3	0.94
Mass, g	21.01
Hardness (Shore A)	55
Operating temperature, °C	-30...+100
Conditional tensile strength, MPA	14.7
Recovery rate	0.68

Perforated sifting surfaces

For the PSS study we chose two variants of rectangular flat plates with round holes (Fig. 3a) and holes of complex geometry in the form of an epicycloid (Fig. 3b). For the study, we selected design parameters that are typical for the industrial production of perforated surfaces by mechanical stamping. In this case, the edge of the holes makes an angle of 90 degrees, which is also optimal for sifting bulk material particles. However, if necessary, the edge angle can be changed and the analytical model adjusted.

The conducted studies [4, 7, 24] proved that the use of PSS with holes of complex geometry can significantly increase the sifting of particles of loose materials through the holes. This is due to the elimination of natural defects in the shape in the form of bulges and depressions, as well as the intensity of cleaning or unblocking of holes by reducing the contact area between the loose material particle and the edge of the holes. So, a particle of loose material will have a different contact area with the edges of the basic holes (Fig. 4a, 4b) and epicycloid holes (Fig. 4, c–f) with a different number of petals or modules. It is obvious that the maximum contact area of the

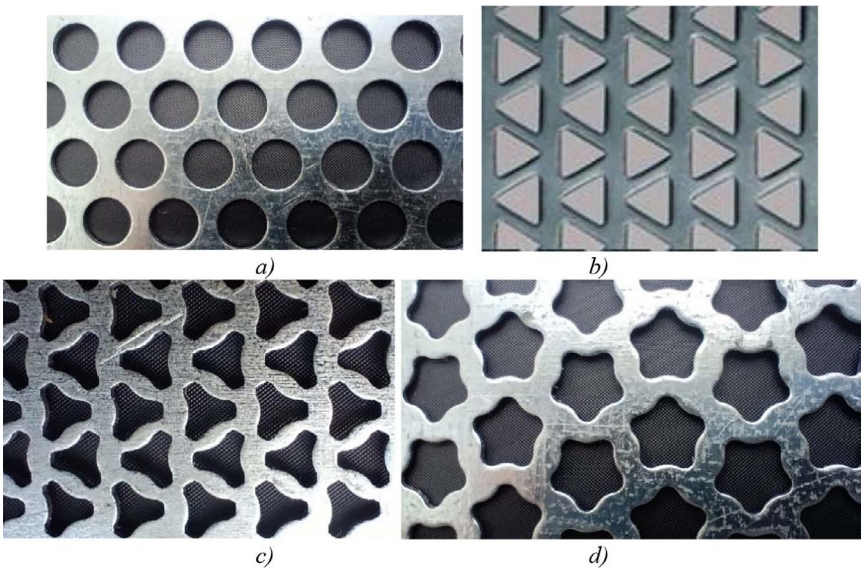

Figure 3. General view of perforated sifting surfaces with basic round (a) and triangular (b) holes, holes of complex geometry in the form of epicycloids (c, d)

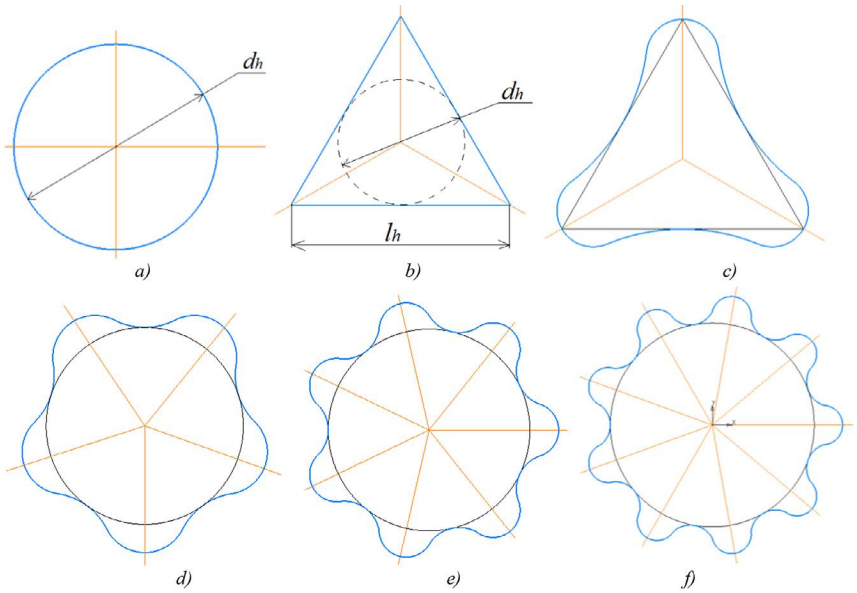

Figure 4. Diagrams of holes of perforated sifting surfaces: *a* – basic round; *b* – basic triangular; *c, d, e, f* – holes of complex geometry in the form of epicycloids (three-petaled, five-petaled, seven-petaled and nine-petaled, respectively)

loose material particle with the edges is observed for round and triangular PSS holes (Fig. 4a, 4b), and the use of the epicycloid form of the hole will significantly reduce this contact area. At the same time, the variation in the number of petals in epicycloid holes (Fig. 4 b–e) additionally leads to a change in the contact area, and, accordingly, the force of adhesion. For the study we used PSS made of still S235 JR steel with the following parameters (Table 2).

Particles of loose materials and their properties

For the study we selected loose materials of biological origin, such as grains of wheat, corn, peas, buckwheat (Fig. 5). To take into account the geometric parameters in particles of loose materials of biological origin, they are divided into two groups: those of rounded shape (Fig. 5, a) and those in the form of a tetrahedron (Fig. 5, b). Such a choice of particles and their shapes allows us to study and further use the results for most types of loose materials.

We used generally accepted method of microscopy to determine the dimensional characteristics [25, 26]. The study was performed on an Opta-tech × 2000 microscope (Fig. 6) with the following characteristics: zoom 1:10/0.8 × -8 ×; equipped with a clik-stop mechanism; adjustable eyepiece distance between 45–76 mm; planachromatic lens; field of view 10 × 22 mm; EPI/DIA illuminator brightness adjustment; LED lighting. RADWAG WAS 100/C/2 electronic scales were used to determine the mass of loose material particles (Fig. 7) with the following parameters: accuracy class I, maximum

Table 2. Parameters of perforated sifting surfaces

Type of holes	Hole shape	Type of loose material	Separation size, mm	Surface thickness h_s mm
Basic	Circle	Wheat	R_h=1.5 mm	0.8...1.2
		Peas	R_h=3 mm	
		Corn	R_h=4 mm	
	Equilateral triangle	Buckwheat	L_h= 6mm	
Complex geometry	Three-petaled epicycloid	Buckwheat	R_h= 0.003 m	
	Five-petaled epicycloid	Wheat/ Peas/ Corn	R_h= 1.5 mm/ r_h=3 mm/ r_h=4 mm	
	Seven-petaled epicycloid			
	Nine-petaled epicycloid			

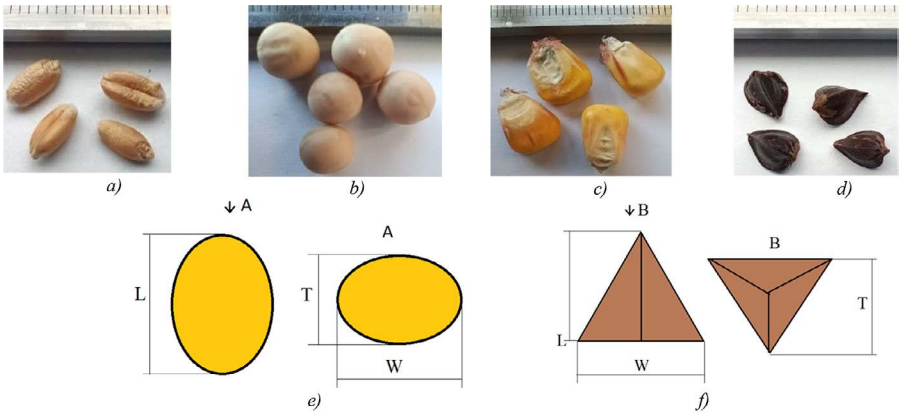

Figure 5. Particles of loose materials and their geometric parameters: *a* – wheat; *b* – peas; *c* – corn; *d* – buckwheat; *e* – diagram of the size of rounded particles; *f* – diagram of the size of particles in the form of a tetrahedron

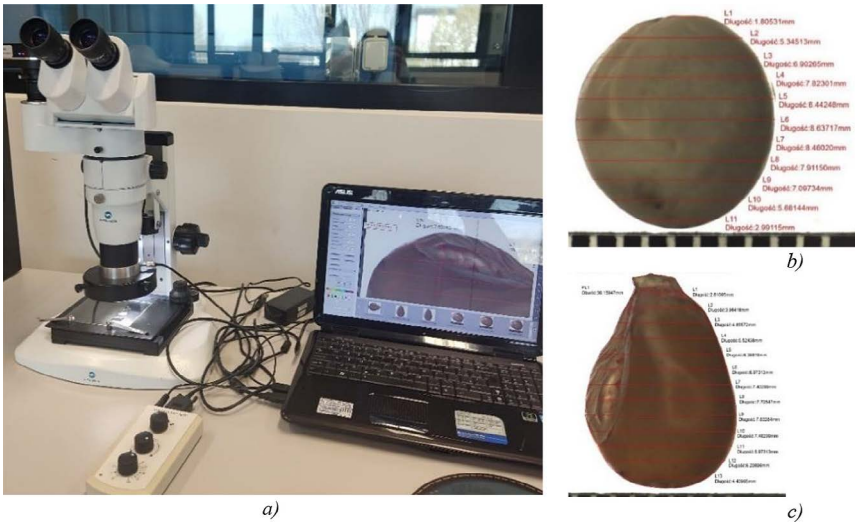

Figure 6. Microscopy of loose material particles: *a* – general view of the Opta-tech × 2000 microscope; *b*, *c* – image of pea and corn particles, respectively

load 100 g, measurement interval 0.1 mg. The difference between particles of loose materials of biological origin and others, such as those for construction purposes, is anisotropy and their moisture level. These properties determine the level of particle elasticity and should be taken into account in our studies. One of the values that characterize the ability of a material to resist external loads within elastic deformation is the longitudinal elasticity coefficient of the 1st grade (Young's modulus).

To determine the modulus of elasticity of particles of loose material of biological origin, we used the basic method [27, 28], which provides for: static compression of pre-prepared particles of different moisture of the installation between the tip of the micrometer indicator head and the helical moving platform. For this purpose, we used the AGW-3 Digital

Figure 7. Laboratory equipment for determining the mass of loose material particles

Figure 8. Digital pressure gauge (Tester AGW-3): 1– digital unit; 2 – pressure head; 3 – loading platform; 4 – flywheel of the platform; 5 – base; 6 – column

pressure gauge (Fig. 8) with the following characteristics: maximum load 196 N; Force sensitivity 0.1 N; platform relative velocity 0.25 mm/s; platform diameter 17.5 mm; measurement accuracy ± 2%. Typical force deformation curve (Fig. 9) has characteristic points: A – partial destruction of the shell (upper protective layer); B – the point of maximum force and moment of destruction of the particle.

The OA zone has a directly proportional increase in deformation relative to the load. At this stage of loading, the particle retains its elastic properties. The zone near point A corresponds to conditional fluidity, that is, an increase in deformation under constant load. The value of absolute deformation at this moment is insignificant, it equals to hundredths. This is explained by the fact that on the surface of a particle of loose material,

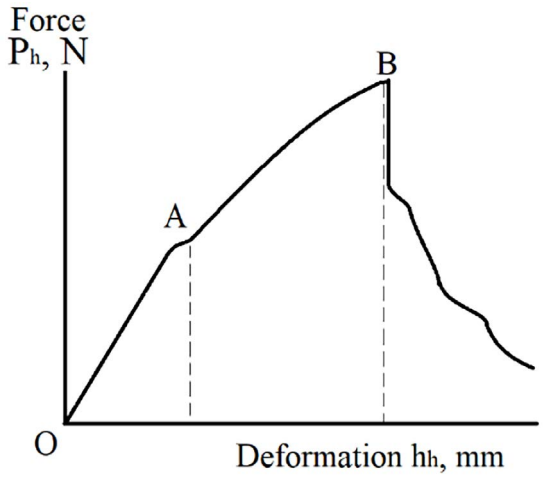

Figure 9. Typical diagram of the destructive force of a loose material particle

the destructive force is distributed over the area, which causes the filling of interlayers in the structure between the shell layers. Places of deformation on the particle surface can be identified as a contact spot by microscopy at 15× magnification. Further increase in the load on the AB zone is characterized by a larger angle of inclination of the curve. The particle retains its elastic properties with little plastic deformation. The load in this zone causes internal cracks and compaction on the surface of the particle in the contact area.

A characteristic feature of Zone B is a significant increase in plastic deformation under constant load. This is due to the internal displacement of the structure. The coordinate of point B itself corresponds to the maximum load (force) at which the particle structure begins to deform with characteristic features, for example, a crack or a chipped part. For the studies we randomly placed a given particle of loose material on the platform (pos. 3, Fig. 8). Next, we rotated the helical flywheel (pos. 4, Fig. 8) as a result, we reduced the distance between the platform (pos. 3, Fig. 8) and the head (pos. 2, Fig. 8), which provided the necessary force on the particle of loose material. Under critical load, the particle shell was destroyed, which was recorded from the block (pos. 1, Fig. 8) as a peak value. In addition, we determined the level of deformation of the loose material particle. For this we performed taring and received the dependence of the flywheel speed (pos. 4, Fig. 8) and vertical movement of the platform (pos. 3, Fig. 8), which made it possible to determine the depth of immersion of the head in a particle of loose material.

The Young's modulus (E) was determined from the obtained values of the external force and the corresponding level of deformation of the loose material particle [29–31]:

$$E = \frac{0{,}886 P_h \psi (1-\nu^2)}{h_h^{\frac{3}{2}} d^{\frac{1}{2}}} \quad (5)$$

where: P_h is the resistance to movement (force) of the head in a particle of loose material, N; ψ is the reduced elastic constant; ν is Poisson's ratio; d – cylindrical head diameter, mm; h_h – depth of immersion of the head in the particle, mm.

The used method provides for establishing the resistance to movement of the head P_h from the side of the loose material particle, taking into account the elastic constant ψ and the Poisson's ratio ν. It should be noted that damage to loose material particles affects the duration of their storage, the quality of further processing products, and the reproductive properties of seed material [32]. For the study we prepared samples of loose material particles with different moisture, which was determined according to a well-known laboratory method, such as grinding, drying, and calculation of mass changes. Experimental samples of particles of loose materials were moistened with the quantity of water determined by the following expression [33]:

$$Q_w = \frac{m_p (M - M_o)}{100 - M} \quad (6)$$

where: Q_w is quantity of added water; m_p is an initial mass of loose material particles, M_0 – actual initial particle moisture; M – the final set moisture of the particles.

All samples of loose material particles are artificially prepared in five moisture variations (M). Then the loose material particles were packed in dense polyvinyl chloride containers and stored for 7 days at 4 °C to ensure homogenization and uniform internal moisture distribution [34, 35]. Particles of loose materials were also selected by pre-sifting on laboratory sieves and separating impurities. Particles of loose material of biological origin can be considered as an asymmetric anisotropic body that contains elements with different properties and chemical composition. In addition, such particles have biological viability and development. Based on this and on the methods of similarity theory, it is proposed to assume an elastic constant comparable to the ratio of linear particle sizes of loose material [36, 37], namely for experimental particles ψ = 1.18–1.34. The value of the Poisson's coefficient, taking into account shells in particles of loose materials and based on known studies [29, 30, 38], is ν = 0.35. Experiments for each type of loose materials were repeated 5 times and averaged, which allowed us to obtain results with a confidence probability greater than p = 0.95.

The movement of loose material particles relative to PSS is accompanied by friction, which must be taken into account in the form of a coefficient f. For the study we used well-known methods of identification of the coefficient of friction of loose material particles on steel [39–42]. To do this, we used the device (Fig. 10) in the form of a flat steel plate, which has the ability to change the angle of inclination. We recorded the beginning of movement of particles of loose material by slowly increasing the angle of inclination of the plate.

The coefficient of friction of loose material particles was determined by the expression [43, 44]:

$$\mu = \tan \alpha \quad (7)$$

where α is the angle of inclination of the steel plate (Fig. 10).

The friction angle of a loose material particle depends on its shape, mass, surface condition, and the properties of the surface with which it comes into contact. The moisture content of the material significantly affects the mass of the particle and, accordingly, the coefficient of friction [39, 45]. The moisture content of the loose material particles varied within M = 5.5–19%.

RESULTS

Results of identification of properties of loose material particles

As a result of microscopy and weighing of experimental samples of loose material particles, we established their average size and mass (Table 3, 4, Fig. 11). The coefficients of friction of particles on steel are also established (Table 4, Fig. 11).

The results of experimental data and certain elastic modulus of experimental particles of loose material are shown in Table 5. Ranges for varying the depth of immersion of the head for experimental particles of loose materials within their moisture made up h_h = 0.1–2.2 mm.

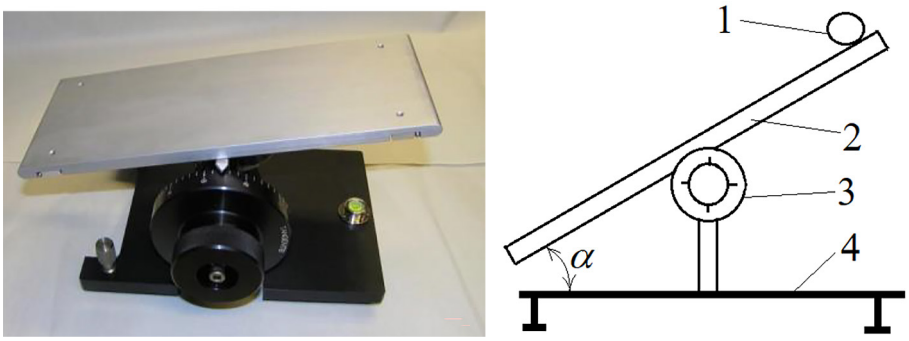

Figure 10. Device for measuring the angle of friction: 1– particle of loose material; 2 – steel plate, 3 – regulator of the angle of inclination of the plate; 4 – base

Table 3. Geometric parameters of loose material particles (mm)

Material type	Length *L*	Width *W*	Thickness *T*
Wheat	5.8 ± 0.08	3.3 ± 0.05	3.2 ± 0.03
Peas	7.05 ± 0.16	6.47 ± 0.18	6.03 ± 0.17
Corn	9.43 ± 0.32	8.15 ± 0.29	5.89 ± 0.17
Buckwheat	6.64 ± 0.15	4.48 ± 0.1	3.71 ± 0.06

Table 4. Mass and friction coefficients of loose material particles (average values)

Type of loose material	Particle moisture *M*, %	Particle mass m_p, 10^{-3} g	Angle of inclination α, degrees	Coefficient of friction *μ*
Wheat	6.1	34.5	21	0.384
	8.1	35	22.5	0.414
	11.5	36	24	0.445
	14	37	26.5	0.499
	16.6	38	29	0.554
Corn	8.1	274	17.5	0.31
	9.2	275	18	0.325
	11.1	277	20.5	0.374
	14.5	281	26	0.488
	19	284	29.5	0.566
Peas	6.4	193	12	0.212
	8.1	195	12.5	0.222
	10.9	198	13.5	0.24
	13.5	202	15	0.268
	16.8	206	17.5	0.315
Buckwheat	5.5	19.5	19	0.344
	7	20.5	20.5	0.374
	11.6	22	23	0.42
	14	24	25.5	0.47
	16	25.5	26.5	0.498

Using expression (5) and experimentally calculated data from the Table 5 we built the graphical dependences of the elastic modulus of loose material particles on their moisture (Fig. 12).

The obtained dependences were approximated using the least squares method:

a) for corn particles $y = 1259.6e^{-0.23x}$; $R^2 = 0.9993$;

b) for pea particles $y = 816.44\ e^{-0.235x}$; $R^2 = 0.9965$;

c) for wheat particles $y = 619.86\ e^{-0.232x}$; $R^2 = 0.9991$;

d) for buckwheat particles $y = 644.96\ e^{-0.3x}$; $R^2 = 0.9909$.

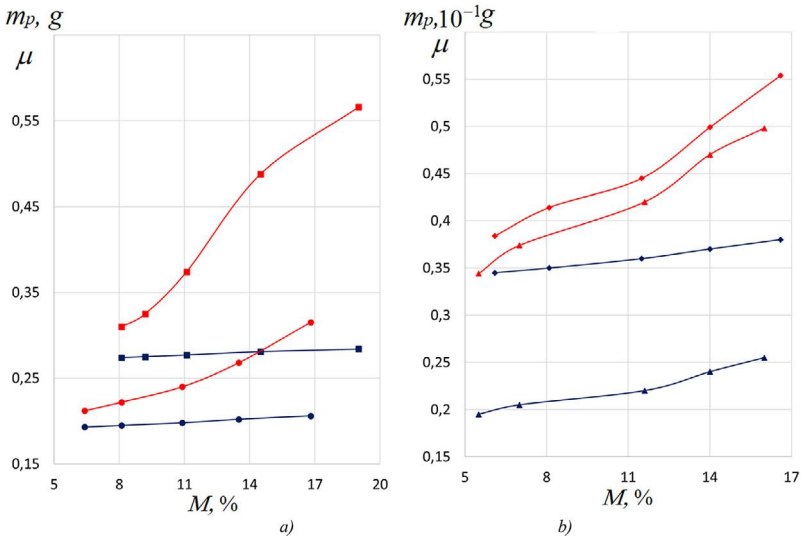

Figure 11. Dependence of mass (m_p) and the coefficient of friction (μ) of particle of loose material from its moisture(M): *a* –corn (–■–) and peas (–●–); *b* – wheat (–◆–) and buckwheat (–▲–); red indicates the coefficient of friction, and blue indicates the mass

An increase in the amount of moisture in the particles of loose materials causes a decrease in elastic properties and, vice versa, an increase in plastic ones. The difference in the internal structure and density of particles, shape and size, the presence of elements (shells, embryos, etc.), leads to variability in the change in the elastic modulus.

Thus, an increase in the moisture of loose material particles in the range of 5.5–19% increases the modulus of elasticity of wheat particles by 11.4 times; peas by 11.7 times; corn by 12.6 times; buckwheat by 15.1 times. Such a significant change in the elastic modulus indicates a significant change in the plasticity of loose material particles and the importance of taking into account the PSS hole clogging when studying.

Analytical determination of the force of adhesion of a loose material particle with the edge of holes of perforated sifting surfaces

When cleaning blocked holes, the PSS elastic ball cleaner (Fig. 2) overcomes the binding force of the loose material particle stuck with the edge of the hole. Let's assume additional constraints and assumptions for modelling. Taking into account the results, let's assume that particles of loose materials of biological origin are an elastic body with appropriate dimensions (Fig. 12). Let's also introduce constructive parameters that characterize PSS (Fig. 13): d_h/l_h – diameter/leg of the hole, h_s – edge thickness.

Let's introduce the following parameters when a loose material particle is clogged (blocked) in the PPS hole: l_1, l_2 – coordinates of the location of the center of the ellipsoid or tetrahedron of the loose material particle in relation to the upper (working) surface of the PSS; a_d – the amount of elastic deformation of the loose material particle; h_d – the length of the path of clogging of the loose material particle. The force of adhesion of a deformed particle of loose material with the edge of the hole, taking into account the above, is determined with allowances made for the friction forces that hold it in the PSS hole:

$$F_{ad} = \mu h_s \int_{(L)} p dL_k \qquad (7)$$

where: μ is a coefficient of friction of loose material particles on PPS (steel) material; h_s – PPS thickness (hole edge); L_k – length of the contact line of the stuck particle with the edge of the hole; $\eth$ – is the pressure formed at the contact area of the loose material particle with the edge of the hole.

The value of the contact line length L_k will depend on the shape of the cross-section of the loose material particle and the shape of the hole:

- for round hole: $\int_{(L)} dL_{kr} = \pi d_h$;
- for triangular hole: $\int_{(L)} dL_{kr} = 3l_h$;
- for a hole of complex geometry in the form of an epicycloid: $\int_{(L)} dL_{kep} = k_e \pi d_h$ or $\int_{(L)} dL_{kep} = k_e 3l_h$.

Table 5. Determination of the Young's modulus of loose material particles

Type of loose material	Particle moisture M, %	Head movement resistance (force) P_h, N	Young's Module E, MPa
Wheat	6.1	95	158
	8.1	84	94
	11.5	60	40
	14	46	24
	16.6	33	13.8
Corn	8.1	73	196
	9.2	51	156
	11.1	53	101
	14.5	57	46
	19	43	15.5
Peas	6.4	92	182
	8.1	81	115
	10.9	69	69.3
	13.5	56	33
	16.8	34	15.6
Buckwheat	5.5	66	121
	7	53	74
	11.6	38	25
	14	36	11.1
	16	34	8

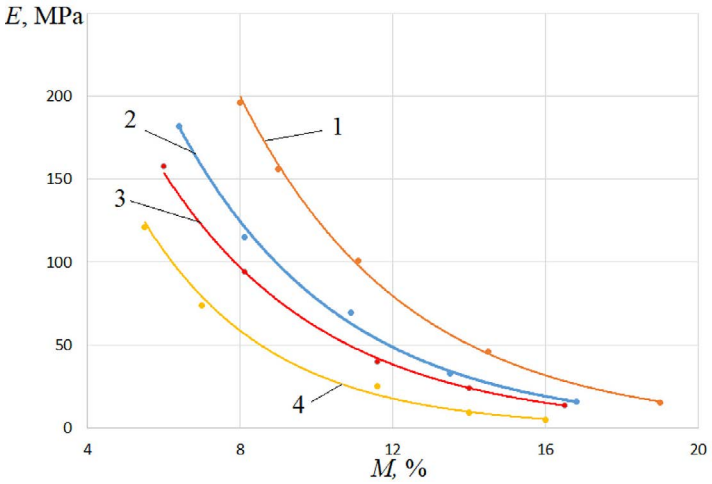

Figure 12. Dependences of the elastic modulus of loose material particles on their moisture: 1 – corn; 2 – peas; 3 – wheat; 4 – buckwheat

where k_e is a contact coefficient, which takes into account the change in the contact area of the loose material particle and the edge of the hole (k_e = 1 – for round and triangular basic holes with the maximum contact area).

For holes of complex geometry, for example, of epicycloid form, the contact coefficient k_e will be significantly smaller than for the basic holes (Fig. 14).

By geometric calculations we established the value of the contact area (red line) between the

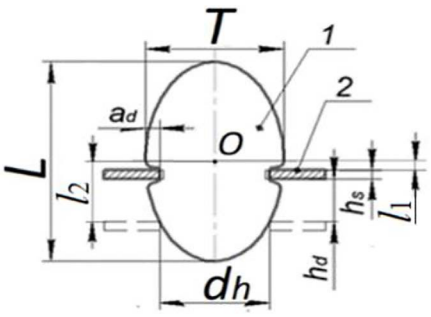

Figure 13. Scheme of clogging of a loose material particle (1) in the hole of a perforated sifting surface (2)

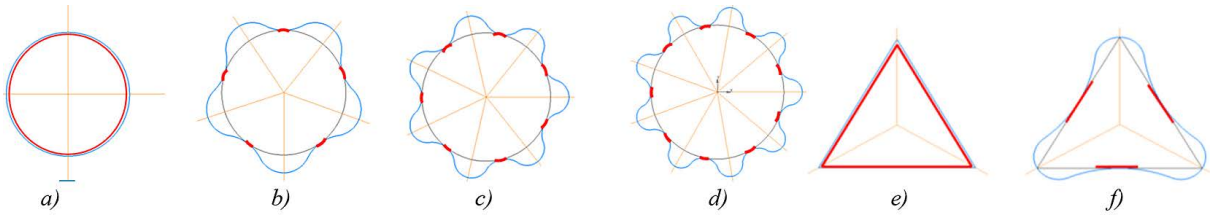

Figure 14. Visualization of changes in the contact area of a loose material particle depending on the type of holes

loose material particle and the edge of the PSS holes, which made it possible to determine the corresponding contact coefficients k_e (Table 6).

To determine a significant parameter, namely the pressure at the contact area of the loose material particle with the edge of the hole, we make the following assumption, which assumes a constant pressure value δ over the entire contact surface area. Also, we note that the pressure δ determines the value of the adhesion force and depends on the value of elastic deformation of the loose material particle a_d. To determine the pressure δ we use generalized Lamet equations, equations of the theory of elasticity in displacements, which relate the value of surface pressure to elastic radial displacements of points [46, 47]:

$$p = \frac{2E}{(1+\nu)(1-2\nu)}\frac{a_d}{R_h} \tag{8}$$

where: E and ν are elastic modulus and Poisson's ratio for a loose material particle.

The value of radial elastic deformation is determined by the geometric dimensional characteristics of loose material particles and the parameters of PSS holes, taking into account the coordinates l_1 and l_2:

$$a_d = \frac{T}{2}\left[\sqrt{1-\left(\frac{2l_1}{L}\right)^2} - \sqrt{1-\left(\frac{2l_2}{L}\right)^2}\right] \tag{9}$$

For small values $\frac{2l_1}{L}$ and $\frac{2l_2}{L}$, which are characteristic of the most prone to clogging particles of loose material, expression (9) can be simplified:

$$a_d \approx \frac{T}{L^2}\left(l_2^2 - l_1^2\right) \tag{10}$$

The coordinate l_2 can be defined from the following expression:

$$l_2 = \frac{R_h L}{T}\sqrt{\frac{T^2}{4R_h^2} - 1} \tag{11}$$

The coordinate l_1 we find from the assumption of equality of the kinetic energy of a moving particle of loose material during its contact with the hole and the deformation resistance forces and the entry of a particle of loose material during its clogging:

$$\frac{k_{ml} m_p V_{rp}^2}{2} = \frac{2}{3}\pi\mu h_s \frac{E}{(1+\nu)(1-2\nu)}(2l_2 + l_1)(l_2 - l_1)^2 \tag{12}$$

where: k_{ml} is the number of sublayers of loose material, which allows to take into account the change in particle weight; m_p is mass of one particle of loose material (Table 4); V_{rp} – relative velocity of the loose material particle at the moment of contact with the hole edge [4, 7, 24, 48].

Number of sublayers k_{ml} equals to the number of particles in the thickness of the loose material layer h (Fig. 1), which moves along the PSS, and is included in the expression:

$$h = k_{ml} T \tag{13}$$

where: T is the thickness of the particle of loose material.

Table 6. Dependence of coefficients of contact k_e on the type of holes of perforated sifting surfaces

Hole shape	Image in Figure 13	Coefficient k_e
Round	a	1
Triangular	b	1
Three-petaled epicycloid	c	0.27
Five-petaled epicycloid	d	0.11
Seven-petaled epicycloid	e	0.16
Nine-petaled epicycloid	f	0.21

For the study assume that sublayers 1, 2 and 3 that correspond to the thickness of loose material particles and characterize the specific load on the working bodies of separation machines [4, 24]. Then, accordingly, we have: for a loose material with a layer thickness of one particle $k_{ml} = 1$, for loose material with two sublayers $k_{ml} = 2$ and with three sublayers – $k_{ml} = 3$. The resulting expression (12) is a cubic equation with respect to l_1. To solve it, we use the Cardano formula [49, 50], which allows to find the roots of a cubic equation in the region of complex numbers. To do this, we transform the cubic equation (12) to the following form:

$$\tilde{N}l_1^3 - 3Cl_1l_2^2 + 2Cl_2^3 - C_1 = 0 \qquad (14)$$

where: $\tilde{N} = \frac{2}{3}\pi\mu h_s \frac{E}{(1+\nu)(1-2\nu)}$; $\tilde{N}_1 = \frac{k_{ml} m_p V_{rp}^{\ 2}}{2}$

are coefficients of the cubic equation;

l_2 is the coordinate determined by (11).

It should be noted that the hole blocking condition provides for: $l_2 \geq l_1$. When we found l_1 and l_2 we proceed to the determination of the force of adhesion by the final expression:

$$F_{ad} = \frac{16\pi\mu h_s k_e T}{L^2} \frac{E}{(1+\nu)(1-2\nu)} \left(l_2^{\ 2} - l_1^{\ 2}\right) \qquad (15)$$

CALCULATION RESULTS

The numerical calculations were conducted for particles of loose material of wheat, corn, peas and buckwheat based on outstanding experimental (Tables 2–6, Fig. 11, 12) and well-known data [51]. We established the dependences of the adhesion force on the moisture content of loose material particles and the PSS thickness (Fig. 15, 16); from the number of sublayers (Fig. 17, 18).

The increase of the thickness of perforated surface (Fig. 14, 15) leads to an increase in the contact area "loose material particle – edge of the PPS hole", which causes an increase in the value of adhesion forces: by 18.42–26.26%. The increase in the moisture content of loose material particles causes a decrease in the values of the adhesion force: by 35–35.3% for buckwheat; by 36.5–36.8% for wheat; by 35.1–37.7% for corn; by 35.4–37.4% for peas.

The increase of the thickness of the loose material layer increases the load (mass) acting on the particle that blocks the PPS hole. For the study range k_{ml} = 1–3 (1, 2 and 3 sublayers) such an increase causes an increase in the value of forces of adhesion: by 41.37–42.14% (Fig. 15, 16).

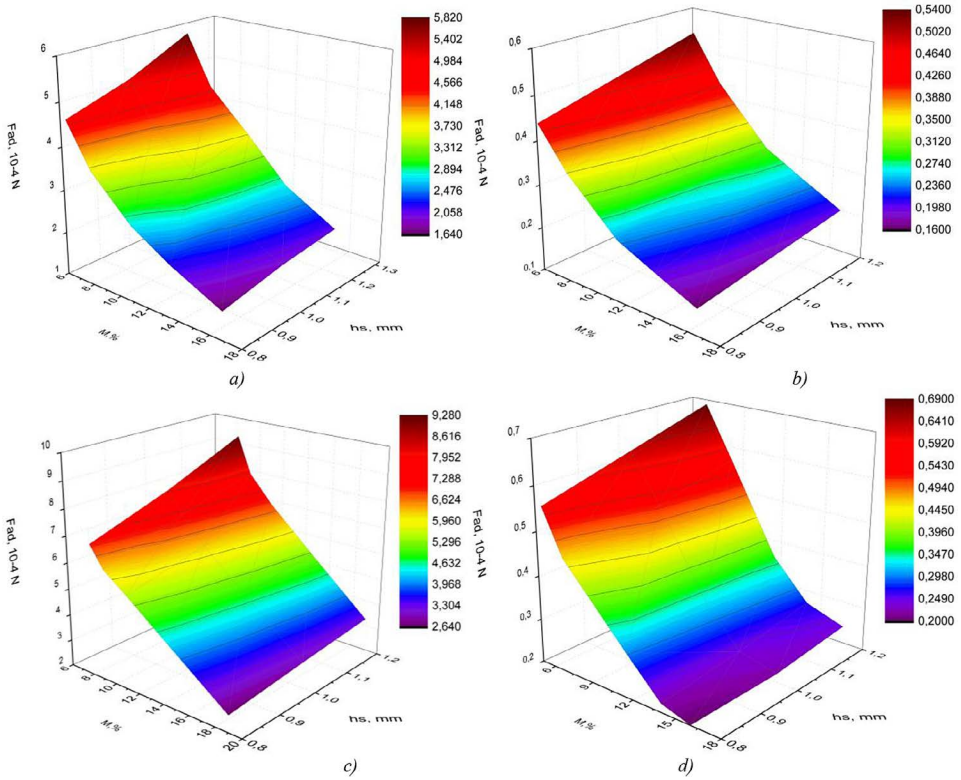

Figure 15. Dependence of the force of adhesion (F_{ad}) from moisture (M) and the thickness of the perforated sifting surface (h_s): *a* – peas; *b* – wheat; *c* – corn; *d* – buckwheat (k_{ml} = 1; V_{rp} = 0.1 m/s; k_e = 1)

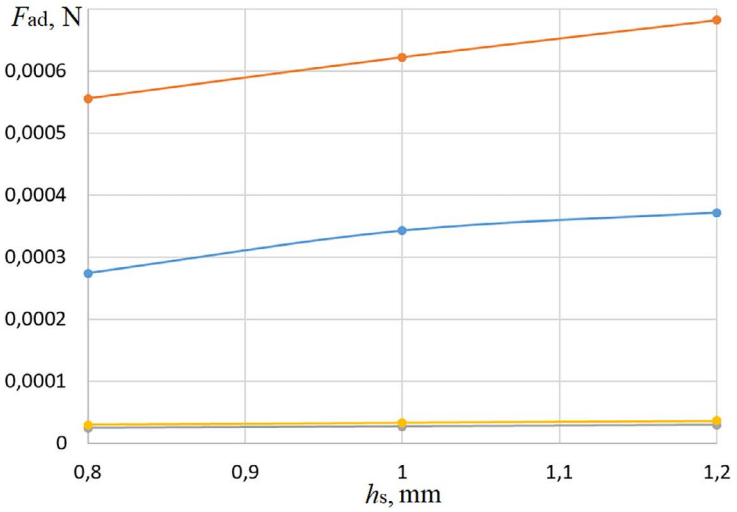

Figure 16. Dependence of the force of adhesion (F_{ad}) from the thickness of the perforated sifting surface (h_s): – peas; – corn; – wheat; – buckwheat; k_{ml} = 1; V_{rp} = 0.1 m/s; k_e = 1; M = 10.9 -11.6%)

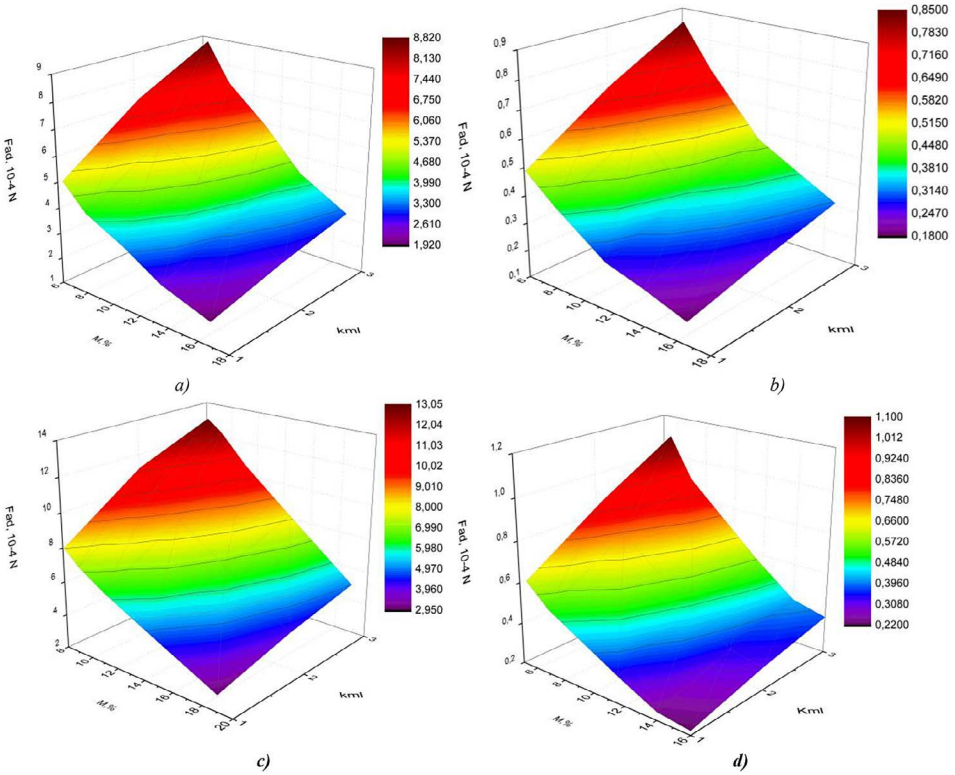

Figure 17. The dependence of the force of adhesion (F_{ad}) from moisture (M) and the number of sublayers of loose material (k_{ml}): *a* – peas; *b* – wheat; *c* – corn; *d* – buckwheat (h_s = 1 mm; V_{rp} = 0.1 m/s; k_e=1)

To determine the effect of the shape of PPS holes on the force of adhesion, we received the corresponding dependences (Fig. 19, 20).

The resulting dependencies (Fig. 20) were approximated using the least squares method: a) for corn particles y = 0.0006x (R^2 = 1); b) for pea particles y = 0.0003x (R^2 = 1); c) for wheat particles y = 3E – 0 x + 2e-07 (R^2 = 0.9996); d) for buckwheat particles y = 3E – 05x + 2e-07 (R^2 = 0.9996). By accepting the contact coefficient for basic holes (round and triangular in shape) k_e = 1 of Figure 20 we see that the use of sieves with holes of complex geometry significantly reduces the adhesion force: by 4.76 times for holes in the form of a 9-petaled epicycloid (k_e = 0.21); by 6.25 times for 7-petaled epicycloids (k_e = 0.16); by 9.1 times for 5-petaled epicycloids (k_e = 0.11); by 3.44 times for 3-petaled epicycloids (k_e = 0.27).

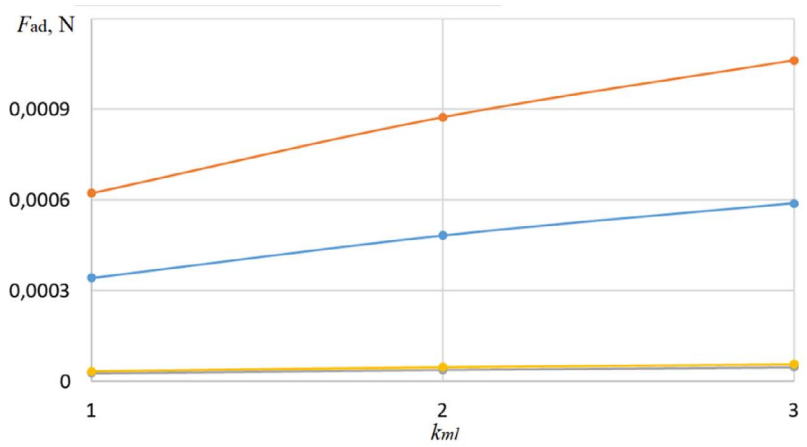

Figure 18. Dependence of the force of adhesion (F_{ad}) from the number of sublayers of loose material (k_{ml}): – peas; – corn; – wheat; – buckwheat; h_s = 1 mm; V_{rp} = 0.1 m/s; k_e = 1; M = 10.9–11.6%)

The velocity of movement of loose material particles as they pass through the holes also affects the value of adhesion force (Fig. 21, 22).

Having investigated the effect of increasing the velocity of a loose medium particle in the range of V_{rp} = 0.05...0.15 m/s (Fig. 21, 22) we found that the adhesion force increases by 2.92–3 times, and its variation ranges are: peas $F_{ad} = 9.48 \times 10^{-5} – 7.7 \times 10^{-4}$ H; corn $F_{ad} = 15.2 \times 10^{-5} – 11.7 \times 10^{-4}$ H; wheat $F_{ad} = 9.1 \times 10^{-6} – 7.4 \times 10^{-5}$ N; buckwheat $F_{ad} = 1.1 \times 10^{-5} – 9.4 \times 10^{-5}$ N. For example, let's determine the parameters of ball cleaners (Table 1) by expression (4), which defines the conditions for holes unblocking for given particles of loose material. For calculations, we assume the established properties of loose material particles (Tables 3–5). We adopt the length of the clogging path of a loose material particle: $\Delta l = l_2 – l_1$, where we calculate l_1 from the expression (14), and l_2 by expression (11). We determine

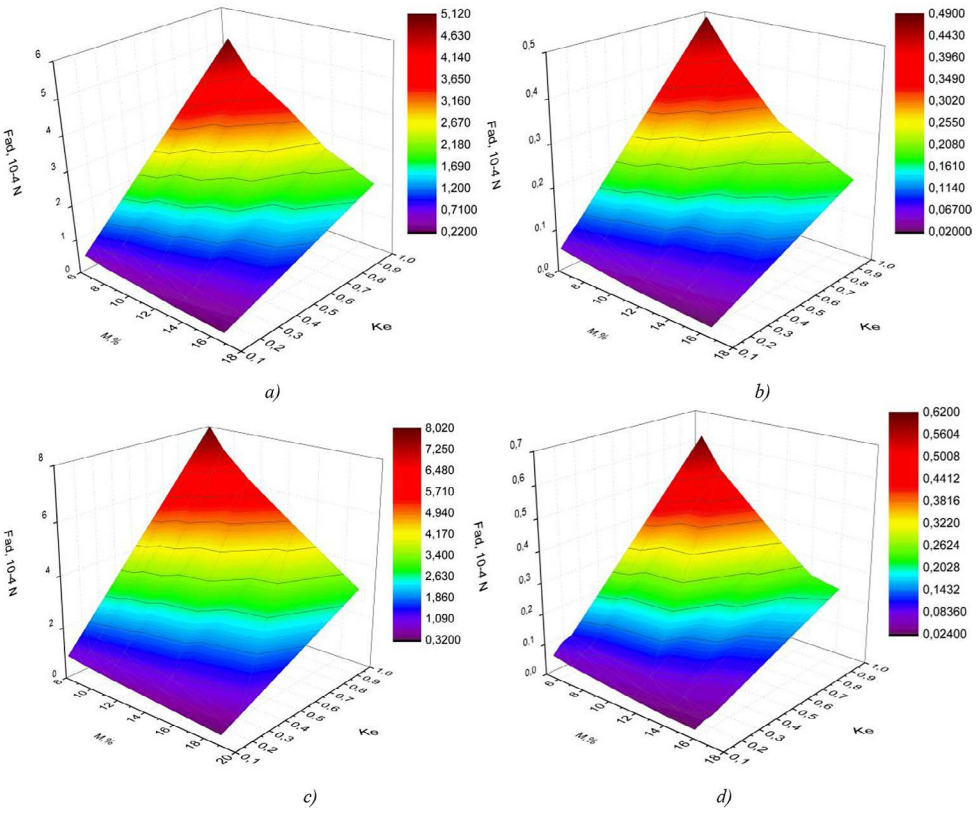

Figure 19. Dependence of the force of adhesion (F_{ad}) from the moisture of the loose material (M) and the contact coefficient (k_e): *a* – peas; *b* – wheat; *c* – corn; *d* – buckwheat (k_{ml} = 1; h_s = 1 mm; V_{rp} = 0.1 m/s)

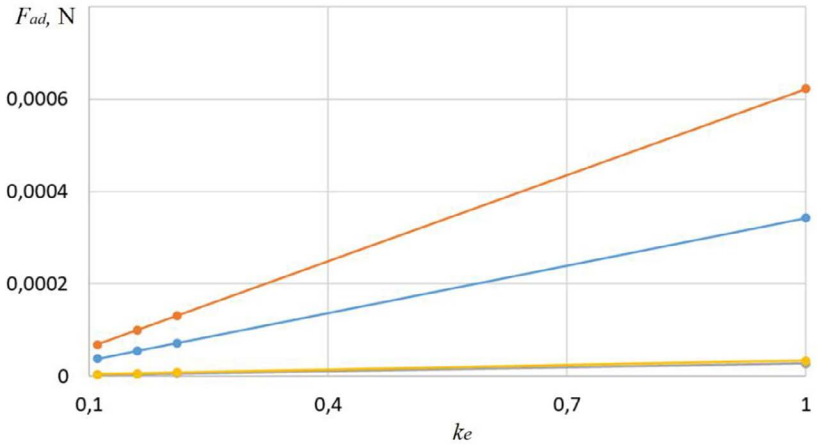

Figure 20. Dependence of the force of adhesion (F_{ad}) from the contact coefficient (k_e): - peas; - corn; - wheat; - buckwheat (h_s = 1 mm; V_{rp} = 0.1 m/s; k_{ml}=1; M = 10.9 – 11.6%)

the force of adhesion F_{ad} using the expression (15) and enter the results in the Table 7. The results presented in Table 7 have the following purpose – to calculate, according to the developed methodology, variants of the parameters of impact elastic cleaner balls. The important result is not the established values, but their difference for different bulk materials. This proves the prospects of using this methodology to optimize the parameters of elastic cleaners of perforated sieving vibrating surfaces. The set values of the ball's velocity (Table 7) are minimum values that ensure the equality of condition (4). The increase of the ball velocity or its mass will ensure that the hole is unblocked from stuck particles of loose material under study. It is established that if the balls have the same mass, their velocity differs depending on the type of particles of loose material and their properties. So, the required velocity of the ball for unblocking holes

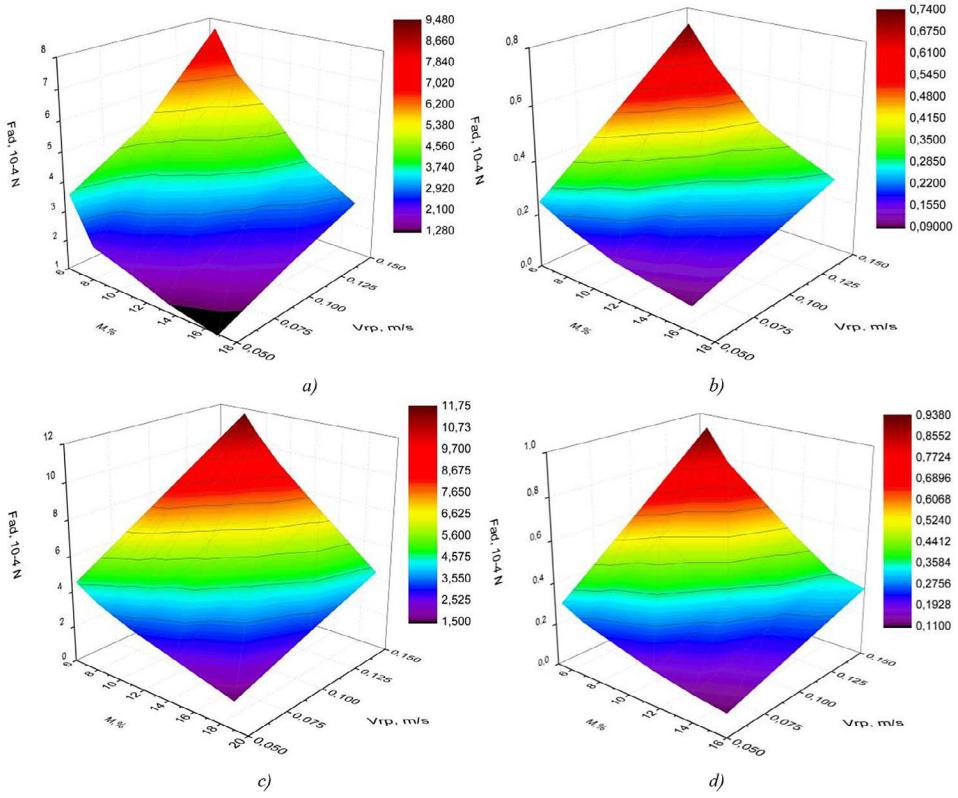

Figure 21. Dependence of the force of adhesion (F_{ad}) from moisture (M) and the velocity of movement of the loose material particle (V_{rp}): *a* – peas; *b* – wheat; *c* – corn; *d* – buckwheat (k_{ml} = 1; h_s = 1 mm; k_e = 1)

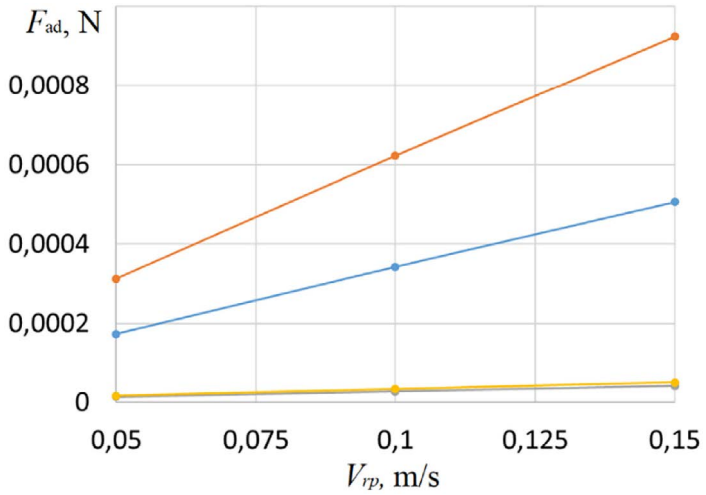

Figure 22. Dependence of the force of adhesion (F_{ad}) on the velocity of the loose material particle (V_{rp}): – peas; – corn; – wheat; – buckwheat (h_s = 1 mm; k_{ml} = 1; M = 10.9 – 11.6%)

Table 7. Parameters of the cleaner ball when unblocking the hole(V_{rp} = 0.1 m/s; h_s = 1mm; k_{ml} = 1; k_e = 1; M = 10.9 – 11.6%)

Material type	l_1, mm	l_2, mm	Δl, mm	Force of adhesion $F_{ad}\cdot10^{-4}$, N	Ball mass m_b, G	Ball velocity V_{rb}, mm/s
Peas	1.312	1.365	0.0534	3.42	21	1.319
Corn	0.849	0.901	0.0512	6.22		1.751
Wheat	1.185	1.208	0.0232	0.27		0.245
Buckwheat	1.652	1.673	0.0201	0.33		0.252

from pea and corn particles is 5.4–6.9 times higher than for wheat and buckwheat particles.

The next stage of study is a comprehensive justification of the parameters of the ball (mass, size, density, coefficient of recovery) and the bumper, which is based on the identified values of the forces of adhesion of loose material particles with the edges of PPS holes.

CONCLUSIONS

1. Based on the analysis of known results and conducted studies, we determined the conditions for blocking holes of perforated sifting surfaces taking into account their parameters, properties of loose materials, and parameters of ball cleaners.
2. It is established that a significant factor in the phenomenon of blocking the hole is the force of adhesion of a particle of loose material with the edges of the hole. For its identification, we developed a method with analytical definitions and experiments taking into account: the size, mass, friction constant and Young's modulus of loose material particles; the shape and dimensions of the hole, the thickness of the perforated sifting surface; the layer thickness and velocity of loose material.
3. Using analytical and experimental methods, we identified variation range of these factors for loose material particles of biological origin, such as buckwheat, wheat, peas, corn.
4. By studies we established the dependence of the force of adhesion on moisture and thickness of loose material layer, as well as thickness and shape of the holes of the perforated surfaces. We have also established the dependence of constant of friction, mass, Young's modulus from the moisture of particles of loose material. The obtained results make it possible to determine the force of adhesion and forecast the power necessary for unblocking this hole, created by the cleaning system elements, such as brushes and elastic impact cleaners.
5. The use of the method will allow us to justify the parameters of the hole cleaning system for perforated sifting surfaces with different types of holes and when separating different types of loose materials according to the criteria of maximizing sifting efficiency and minimizing damage.

Acknowledgments

The authors acknowledge the financial support of the National Science Centre in Krakow to the research project funded in the „POLONEZ BIS 2" call No. 2022/45/P/ST8/02312 entitled Numerical-experimental analysis of a sieve holes' shape and arrangement effect on the degree. POLONEZ BIS is operated by the Centre on the basis of the Grant Agreement No. 945339 concluded with the European Research Executive Agency.

REFERENCES

1. Obraniak A, Gluba T. A model of granule porosity changes during drum granulation. Physicochemical Problems of Mineral Processing 2011, 46: 219–228.
2. Obraniak A, Gluba T. Model of energy consumption in the range of nucleation and granule growth in drum granulation of bentonite. Physicochemical Problems of Mineral Processing 2012, 48. 1: 121–128.
3. Makinde O, Ramatsetse B, Mpofu K. Review of vibrating screen development trends: Linking the past and the future in mining machinery industries. International Journal of Mineral Processing 2015, 145: 17–22, https://doi.org/10.1016/j.minpro.2015.11.001
4. Kharchenko S, Kovalyshyn S, Zavgorodniy A, Kharchenko F, Mikhaylov Y. Effective sifting of flat seeds through sieve. INMATEH-Agricultural Engineering 2019, 58(2): 17–26. https://doi.org/10.35633/INMATEH-58-02
5. Peng L, Feng H, Wang Z, Wang H, Yang H, Huang H. Screening mechanism and properties of a cantilevered vibrating sieve for particles processing. Appl. Sci. 2019, 9: 4911. https://doi.org/10.3390/app9224911
6. Dong K, Esfandiary AH, Yu AB. Discrete particle simulation of particle flow and separation on a vibrating screen: Effect of aperture shape. Powder Technology 2017, 314: 195–202. https://doi.org/10.1016/j.powtec.2016.11.004
7. Kharchenko S. Intensification of grain sifting on flat sieves of vibration grain separators. Monograph; Dissa Plus: Kharkiv, 2017, 217.
8. Ławińska K, Wodziński P. Oczyszczanie sit przesiewaczy. Surowce i Maszyny Budowlane 2011, 2, 46–50.
9. Zexin Xu, Yonglei Li, Lipengcheng Wan, Xiang Ma, Jiannong Song, Jinqiu Huang. Optimising the design of ball racks to improve the sorting efficiency of vibrating screen seed cleaners using discrete element method modelling and experiment. Biosystems Engineering 2023, 225: 99–117, https://doi.org/10.1016/j.biosystemseng.2022.12.006
10. Ławińska K, Modrzewski R. Metody oczyszczania sit przesiewaczy przemysłowych. Technologia i Jakość Wyrobów 2016, 61: 80–85.
11. Ławińska K, Modrzewski R. Przesiewanie i maszyny przesiewające z uwzględnieniem procesu blokowania otworów sitowych: monografia IPS, 2016.
12. Kharchenko S., Samborski S., Kharchenko F. Factors of technological efficiency and reliability of elastic cleaners of vibrating sieves. Proceedings of WECM'23, Pisa, September 2023, 20–22.
13. Ławińska K. Proces blokowania otworów sitowych przesiewaczy stosowanych w przeróbce mechanicznej kopalin użytecznych. Technologia i Jakość Wyrobów 2015, 60: 68–75.
14. Ławińska K, Remigiusz M, Piotr W. Mathematical and empirical description of screen blocking. Granular Matter 2016, 18: 13. https://doi.org/10.1007/s10035-016-0622-4
15. Piecuch T, Pekarski J, Malatyńska G. The equation describing the filtration process with compressible sediment accumulation on a filter mesh. Archives of Environmental Protection. 2013, 39(1): 93–104.
16. Gawenda T. Comparative analysis of mobile and stationary technological sets for screening and grinding. Annual Set the Environment Protection 2013, 15.
17. Feller R. Screening analysis considering both passage and clogging. Trans. ASAE. 1980, 23(4): 1054–1056.
18. Zavgorodny A. Sieve cleaning in grain-cleaning machines: monograph. Kiev: USDA, 1992, 179.
19. Zavgorodny O. Scientific bases of the processes of cleaning the sieve holes of grain cleaning machines: monograph. Kharkiv: Osnova, 2001, 163.
20. Romanyuk N, Ednach V, Bondarenko D, Tikhonov E, Karnaukhov A, Butenko A, Sokolova V. Improvement of devices for cleaning sieves of grain cleaning machines. AIP Conference Proceedings. 2022, 2767: 020005. https://doi.org/10.1063/5.0127256
21. Zavgorodny A, Dyundik S, Romanov V. On the influence of the working bodies of cleaners on the throughput capacity of sieves. Technology of production and design of agricultural machinery 1997, 70–78.
22. Li Y, Xu Z, Wan L, Zhao H, Chen H, Song J. Impulsive force simulation of the rubber ball sieve-cleaning device for batch seed cleaners. Transactions of the Chinese Society of Agricultural Engineering 2021, 37(20): 23e33. https://doi.org/ 10.11975/j.issn.1002-6819.2021.20.003
23. Zexin Xu, Yonglei Li, Lipengcheng Wan, Xiang Ma, Jiannong Song, Jinqiu Huang. Optimising the design of ball racks to improve the sorting efficiency of vibrating screen seed cleaners using discrete element method modelling and experiment. Biosystems Engineering 2023, 225: 99–117, https://doi.org/10.1016/j.biosystemseng.2022.12.006
24. Tishchenko L, Kharchenko S, Kharchenko F, Bredykhin V, Tsurkan O. Identification of a mixture

of grain particle velocity through the holes of the vibrating sieves grain separators. Eastern-European Journal of Enterprise Technologies 2016, 2(80): 63–69. https://doi.org/10.15587/1729-4061.2016.65920

25. Kaliniewicz Z, Grabowski A, Liszewski A, Fura S. Analysis of correlations between selected physical attributes of Scots pine seeds. Technical Sci. 2011, 14(1): 13–22.
26. Method for identifying the sizes and shapes of biological objects / S. Kharchenko, S. Samborski, F. Kharchenko, I. Korzec: WECM'23, Pisa, September 2023, 20–22.
27. Trotsenko V, Trotsenko I. Ways to reduce mechanical damage of barley for mechanical processing. Journal of Physics: Conference Series. 2019, 1260: 112030. doi.org/10.1088/1742-6596/1260/2/022003
28. Zhang H, Liu X, Liu S, Jiang H, Xu C, Wang J. Prediction Model of Dry Fertilizer Crushing Force Based on P-DE-SVM. ACS Omega 2021, 6(5): 3612–3624. doi.org/10.1021/acsomega.0c05120
29. Rozhkovsky M. To determine the mechanism of deformation and destruction of grain materials. Bulletin of Agricultural Science 2000, 7: 50–53.
30. Bo W, Jun W. Mechanical properties of maize kernel horny endosperm, floury endosperm and germ. International Journal of Food Properties 2019, 22(1): 863–877.
31. Trotsenko V, Trotsenko I, Komendantova N, Babariko A. The grain parameters determination based on elements of the elasticity theory. IOP Conf. Series: Earth and Environmental Science 2021, 659: 012065. doi:10.1088/1755-1315/659/1/012065
32. Kharchenko S, Pankova O, Kharchenko F, Syrovytskyi K, Shulyak M, Zubko V, Sokolik S. Scientific and technical substantiation of technology for improving the biopotential of crops: monograph, Kharkiv 157, 2023.
33. Nader J, Assaf JC, Debs E, Louka N. Innovative Method for Determining Young's Modulus of Elasticity in Products with Irregular Shapes: Application on Peanuts. Processes 2023, 11: 2532. https://doi.org/10.3390/pr11092532.
34. Özarslan C. Physical properties of sweet corn seed (*Zea mays saccharata* Sturt.). J. Food Eng. 2006, 74: 523–528.
35. Gorji A, Rajabipour A, Tavakoli H. Fracture Resistance of Wheat Grain as a Function of Moisture Content, Loading Rate and Grain Orientation. Aust. J. Crop Sci. 2010, 4: 448–452.
36. Bakharev D, Volvak S, Pastukhov A. Bionic principles of designing threshing and separating systems for corn cobs: monograph. Publishing House of FSBEI HE, Maysky village, 2018, 168.
37. Bakharev D, Pastukhov A, Volvak S, Dobrickiy A. Methodology and results of experimental determination of corn grain elasticity modulus. Engineering for rural development 2021. Jelgava, 26.–28.05.2021. doi. org/10.22616/ERDev.2021.20.TF019
38. Fei D, Wu YZ, Han ZS, Zhang FW. Experiment on Poisson's ratio determination about corn kernel. Proceedings of 3rd International Conference on Chemical Engineering and Advanced, Trans Tech Publications, 2013, 781–784, 799–802, Switzerland.
39. Kaliniewicz Z, Markowski P, Anders A, Jadwisieńczak K. Frictional properties of selected seeds. Technical Sciences 2015, 18(2): 85–101.
40. Jouki M, Khazaei N. Some Physical properties of rice seed (*Oriza sativa*). Res. J. Appl. Sci. Eng. Technol. 2012, 4(13): 1846–1849.
41. Riyahi R, Rafiee S, Dalvand MJ, Keyhani A. Some physical characteristics of pomegranate seeds and arios. J. Agric. Tech. 2011, 7(6): 1523–1537.
42. Kabas O, Yilmaz E, Ozmerzi A, Akinci İ. Some physical and nutritional properties of cowpea seed (*Vigna simensis* L.). J. Food Eng. 2007, 79: 1405–1409.
43. Kaliniewicz Z. Analysis of frictional properties of cereal seeds. African Journal of Agricultural Research 2013, 8: 5611–5621. doi.org/10.5897/AJAR2013.7361.
44. Sologubik CA, Campan one LA, Pagano AM, Gely MC. Effect of moisture content on some physical properties of barley. Industrial Crops and Products 2013, 43: 762–767.
45. Stankevych GM, Katz AK, Vasiliev SV, Gaponiuk OI. Characterization of physical and mechanical properties of spelt grain. Scientific Proceedings of Odesa National Academy of Food Technologies 2019, 83, 2: 50–56.
46. Leibenzon LS. Variational Methods for Solving Problems in the Theory of Elasticity. Gostekhizdat, 1943, 286.
47. Simona De Cicco. On the deformation of porous spherical bodies under radial surface traction. Journal of theoretical and applied mechanics 2023, 61, 2: 305–316. https://doi.org/10.15632/jtam-pl/161477
48. Kharchenko S., Samborski S., Kharchenko F., Korzec I., Zubko V. Dynamics of loose medium on vibrosieves with riffles and holes of complex geometry. Proceedings of 5th Polish Congress of Mechanics, Gliwice, September 4–7, 2023.
49. Gorroochurn P. Some laws and problems of classical probability and how Cardano anticipated them. Change 2012, 25(4): 13–20.
50. Lestari K, Pasaribu U, Indratno S, Garminia H. Generating roots of cubic polynomials by Cardano's approach on correspondence analysis. Heliyon 2020, 6: e03998. doi.org/10.1016/j.heliyon.2020.e03998
51. Horabik J, Molenda M. Parameters and contact models for DEM simulations of agricultural granular materials. Biosystems Engineering 2016, 147: 206–225. https:// doi.org/10.1016/j.biosystemseng.2016.02.017